The Performance Analyses of an Induction Motor due to Specified Fault Conditions

Alperen Usudum [1] and Deniz Bolukbas [1,2]

[1] FIGES, Dept. of Electromagnetic Design and Analysis, Istanbul, Turkey
alperen.usudum@figes.com.tr; deniz.bolukbas@figes.com.tr
[2] Okan University, Faculty of Engineering and Architecture, Istanbul, Turkey
deniz.bolukbas@okan.edu.tr

Abstract

The induction motors are being widely used in the industry. With the developments on the computational electromagnetic methods and with the aid of powerful computers, the software tools provided great support to the motor design engineers. At this paper, the design steps of a squirrel cage motor are explained and the performance degradation of the motor due to static eccentricity and broken rotor bars faults is analyzed. ANSYS® Maxwell-2D® and RMxprt® software tools are used for analyses.

1. Introduction

Induction motors are being used in industry for more than 100 years. Despite their low efficiency, they are used in a large scale of areas because of easy and cheap way of production. Since many years, the design methods are developed well enough and motor types are standardized. Although developments on increasing the efficiency are continuing, these works are mostly related on material science and production technique improvement. Computer modeling tools are useful to predict the performence of the motor before it's produced. These tools allow multiple design iterations to be done fast at low cost, create new designs and even give the possibility to understand the performance degradations due to some defects. The motor parameters and characteristics can be accurately calculated and predicted in terms of field computation and analysis results.

In this paper, ANSYS Maxwell-2D and RMxprt software tools are used to create a squirrel cage motor design and to analyze the effects of some specified faulty conditions. The analyses are performed with a computer which the specifications are listed in Table 1.

Table 1. Specifications of the computer used for the analyses

Computer Platform:	Processor:	8 Core - intel i7 3632QM
	Ram:	6 GB DDR3 1600 Mhz
	Graphics:	Nvidia Gforce GT 645M

The number of mesh elements and the simulation time required are listed in Table 2.

Table 2. The number of mesh elements and the simulation time

	Number Of Mesh Elements	Simulation Time (hh:mm:ss)
Healty Motor	36456	02:18:44
Eccentric Motor	40276	03:09:17
Two Broken Bars	38260	02:25:05
Four Broken Bars	35498	approx. 04:00:00

The rest of the paper is organized as follows. In Section 2, designing the 112M Frame 5 kW three-phase squirrel-cage induction motor by using RMxprt and Maxwell-2D is explained. In Section 3, three types of faulty conditions, i.e. static eccentricity, two broken rotor bar situation and four broken rotor bar situation is simulated and the results are presented in the relevant subsections. The conclusions are presented in Section 4.

2. Motor Design with ANSYS RMxprt® and Maxwell®

ANSYS Maxwell® is the commercial electromagnetic field simulation software for engineers who are working for designing and analyzing 3-D and 2-D electromagnetic and electromechanical devices, including motors, actuators, transformers, sensors and coils. RMxprt® is another commercial tool developed by ANSYS which is a template-based electrical machine design tool that provides fast, analytical calculations of machine performance and 2-D and 3-D geometry creation for detailed finite element calculations in ANSYS Maxwell. In addition to providing classical motor performance calculations, RMxprt can automatically generate a complete transfer of the 3-D or 2-D geometry, including all properties, to Maxwell for detailed finite element analysis calculations. Maxwell and RMxprt are widely used and became an industrial standard [1-3].

2.1. Squirrel Cage Motor Design with RMxprt

Most common AC motors use the squirrel cage rotor. The squirrel cage refers to the rotating exercise cage for pet animals. The motor typically cast aluminum or copper poured between the iron laminates of the rotor. The major portion of the rotor currents flow through the bars and varnished laminates. Very low voltages at very high currents are typical in the bars and end rings; in order to reduce the resistance in the rotor, high efficiency motors generally use copper.

By using RMxprt, a 112M Frame (as defined by IEC 60072-1 standard) 5kW three-phase squirrel-cage induction motor is designed,. The parameters of the motor is given at Table 3.

Table 3. Motor Design Parameter

Parameter	Dimension
Stator Outer Diameter	170 mm
Stator Inner Diameter	103 mm
Stator	36
Stator - Number of Slots	36
Rotor Outer Diameter	101 mm

Rotor - Number of Slots	28
Rotor Inner Diameter	38 mm
Length	140 mm
Number of Poles	4
Voltage	380 V AC 50 Hz

M600-60 material is assigned for laminated steels of rotor and stator. The B-H curve of laminated steel is defined as Grade EN 10106. The rotor bars are selected as aluminum.The windings are copper. The shaft is assigned as ST1010 steel. The user interface of RMxprt is shown in Fig.1.
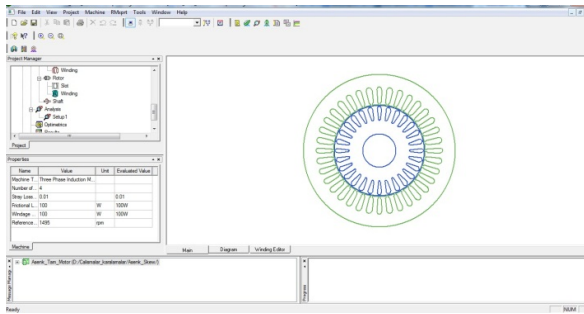

Fig. 1. RMxprt user interface

Since the RMxprt is a template base tool, the time required for analysis is in order of seconds. The results are presented at Table 4.

Table 4. RMxprt results

Number of Revolution:	1399,29 rpm
Stator Phase Current	12,07 A
Stator Resistance	1,0825 Ohm
Torque	34,12 Nm
Total Losses	1158,17 kW
cos ϕ	0,768
Efficiency	81,19%
Output Power:	5,0005 kW

As an output of RMxprt phase current vs speed, torque vs speed, efficiency vs output power and output power vs speed is shown at Fig. 2 (a), (b), (c) and (d) respectively.
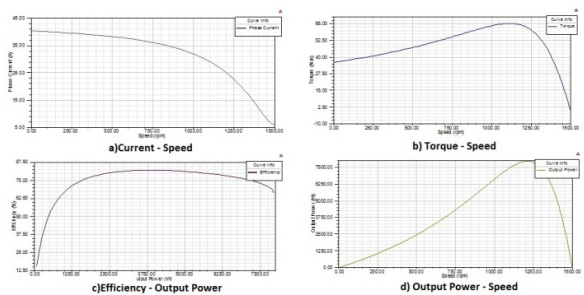
Fig. 2. RMxprt output graphics

2.2. Squirrel Cage Motor Design with Maxwell

The motor specified above is transferred from RMxprt to Maxwell with a direct link. Maxwell uses the accurate finite element method to solve static, frequency-domain, and time-varying electromagnetic and electric fields. At Fig. 3, the user interface of Maxwell-2D and the linkage menu with RMxprt is presented.
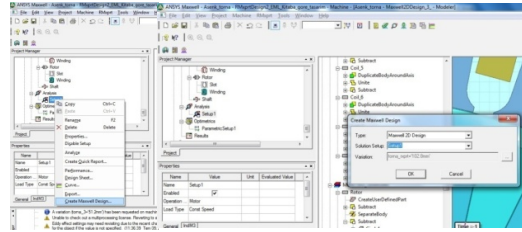

Fig. 3 Maxwell user interface

The parameters of the motor are same, as defined at Table 3. The automatic adaptive meshing technique of Maxwell-2D is used for meshing. Mesh model of motor is shown at Fig. 4.
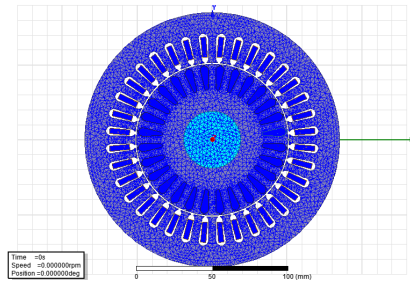

Fig. 4 Mesh model of 112M Frame 5KW three-phase squirrel-cage induction motor.

The motor start up performance is simulated while it's directly connected to network (380 V AC 50 Hz), under the load of 34 Nm during 500 miliseconds with steps of 0,5 miliseconds [4].
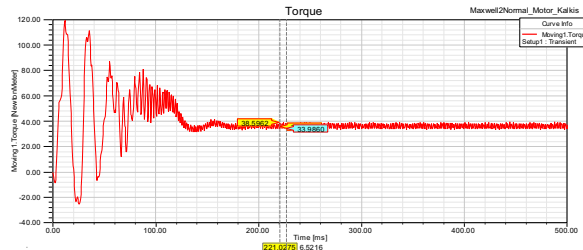
As a result of analysis, the magnetic flux density during the maximum current, the current vs time, torque vs time and speed vs time graphics for the defined motor are obtained and presented at Fig. 5 (a), (b), (c) and (d) respectively.
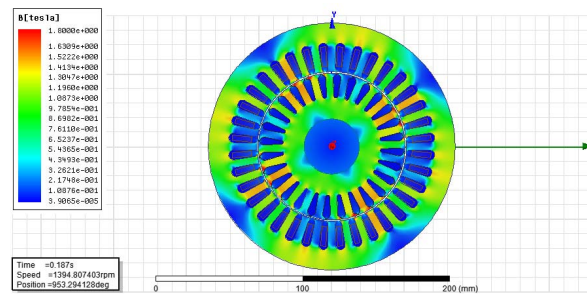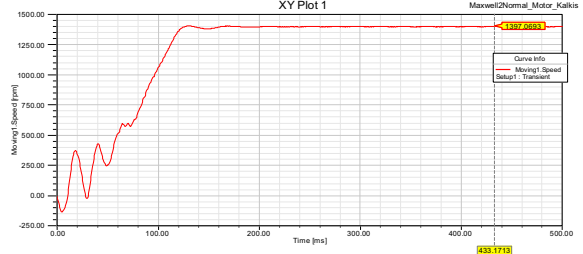

(a) The magnetic flux density during maximum current at nominal working conditions
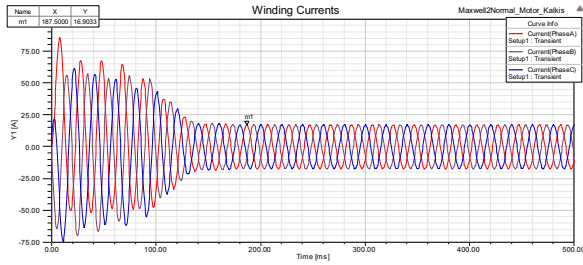
(b) Phase current vs time

(c) Torque vs time graphic

(d) Speed vs time graphic
Fig. 5 The computer simulation results of the healthy motor

As a result of analysis, it is observed that, the motor has reached to nominal working conditions after 150 miliseconds. As it can be seen from the graphics, the motor is able to rotate the 34 Nm load with 1397 rpm and at this working conditions the stator current phase is nominally 11,37 A (rms). These values are compatible with the values at Table 4 which are the results of RMxprt.

3. Analyzing the Faulty Motor

The electric motor is an important element in industrial process in terms of safety and efficiency, the early detection of its malfunctioning is required. The earlier the incipient fault is detected the easier remediable faults will be cheaper. The computer simulations are useful to analyze the faulty conditions. At this section, two fault conditions; i.e. static eccentricity and broken bars, are analyzed and presented.

The motor is directly connected to network (380 V AC 50 Hz), under the load of 34 Nm during 500 miliseconds with steps of 0,5 miliseconds as explained in Section 2.2.

3.1. Analyzing the Static Eccentricity Condition

In a three-phase squirrel-cage induction motor, eccentricity is a common fault that can make it necessary to remove the motor from the production line. Eccentricity results in nonuniform air gap that exists between the stator and rotor. It consists of static, dynamic and a combination of both that is called mixed

eccentricity. In static eccentricity, the rotational axis of the rotor coincides with the symmetrical axis, but it displaces from the stator symmetrical axis. In this case, the air gap distribution is not uniform around the rotor but it is time variant. In this section, the static eccentricity condition is simulated. The stator geometry is shifted 0,75 mm at the direction of x axis. So the rotor is off axis and the air gaps will be in between 0,25 mm and 1,75 mm. The geometry at the Maxwell user interface is shown at Fig. 6.
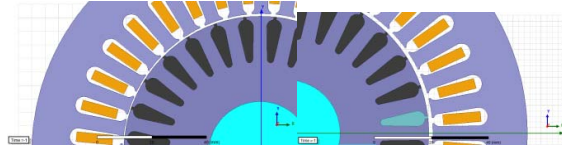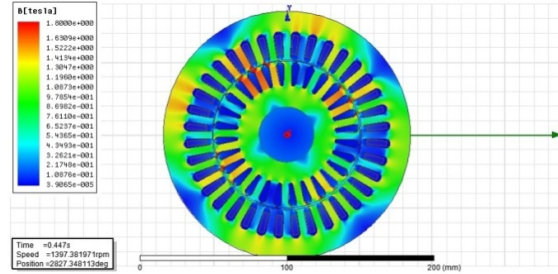

**Fig. 6** The geometry at the Maxwell user interface

The faulty motor with static eccentricity condition is analyzed with Maxwell. As a result of analysis, the magnetic flux density during the maximum current, the current vs time, torque vs time and speed vs time graphics for the defined motor are obtained and presented at Figure 7 (a), (b), (c) and (d) respectively.
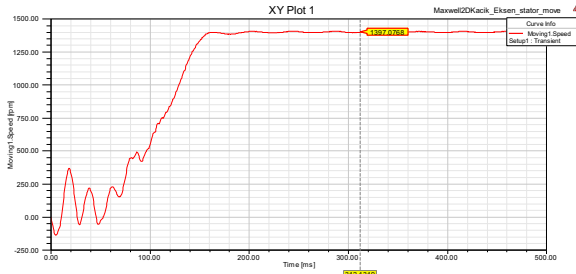

(a) The magnetic flux density during maximum current at nominal working conditions
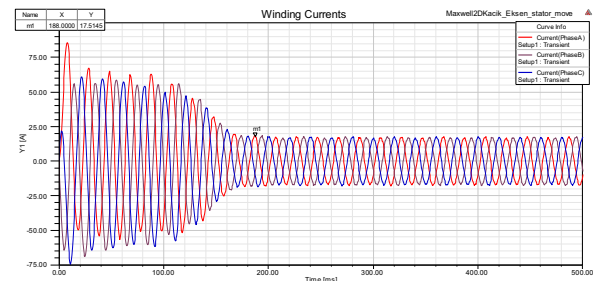
(b) Phase current vs time
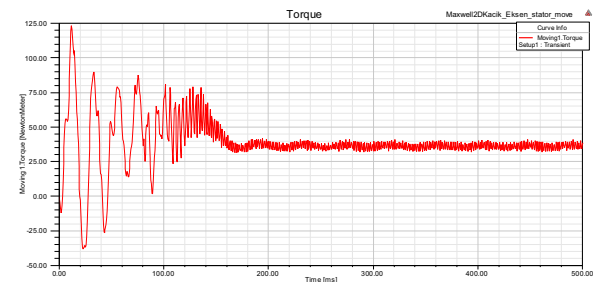
c) Torque vs time graphic

(d) Speed vs time graphic

Fig. 7 The computer simulation result of a static eccentricity condition of the motor

It is observed that, the motor has reached to nominal working conditions after 150 miliseconds. As it can be seen from the graphics, the motor is able to rotate load with 1397 rpm. These figures are same with the healthy motor as explained in Section 2. At this working conditions, the stator current phase is nominally 12,38 A (rms). The fluctuations on the torque and speed graphs may result mechanical vibrations. At Fig. 7 (a), the magnetic saturation areas are observed.

3.2. Broken Rotor Bars

Rotor windings in squirrel cage induction motors are manufactured from aluminum alloy, copper, or copper alloy. Larger motors generally have rotors and end-rings fabricated out of these whereas motors generally have die-cast aluminum alloy rotor cages. Broken rotor bars rarely cause immediate failures, especially in large multi-pole (slow-speed) motors. However, if there are enough broken rotor bars, the motor may not start as it may not be able to develop sufficient accelerating torque. Regardless, the presence of broken rotor bars precipitates deterioration in other components that can result in time-consuming and expensive fixes [5]. A physical example for broken rotor bars is presented at Fig.8.
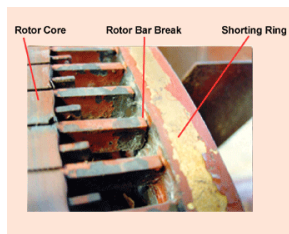

Fig. 8 Broken rotor bars [5]

In this section, the effects of the broken bars are investigated. The analysis are performed with Maxwell 2D, for two broken bars and four broken bars. At Fig. 9, the Maxwell 2D models of the motors with two broken bars and four broken bars, are presented.
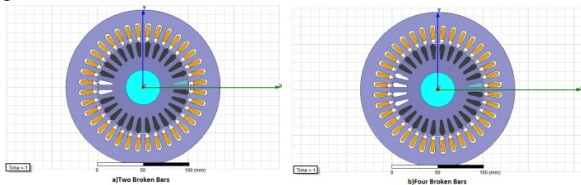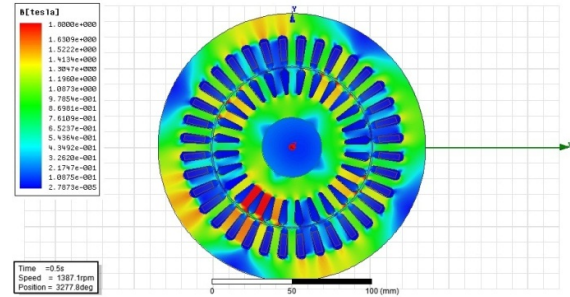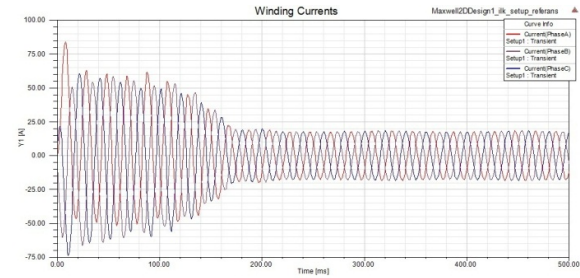

Fig. 9 Maxwell 2D Models of broken rotor bars

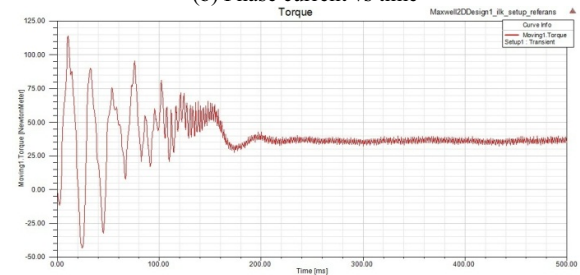### 3.2.1 The effects of two broken rotor bars to the motor performance

The faulty motor with two broken rotor bar is analyzed with Maxwell 2D. As a result of analysis, the magnetic flux density during the maximum current, the current vs time, torque vs time and speed vs time graphics for the defined motor are obtained and presented at Figure 10 (a), (b), (c) and (d) respectively.
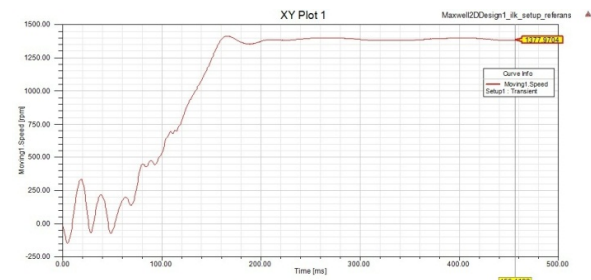

(a) The magnetic flux density during maximum current at nominal working conditions
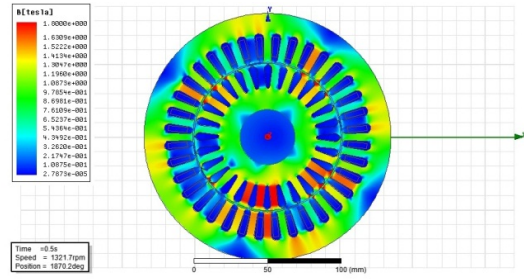

(b) Phase current vs time

c) Torque vs time graphic

(d) Speed vs time graphic

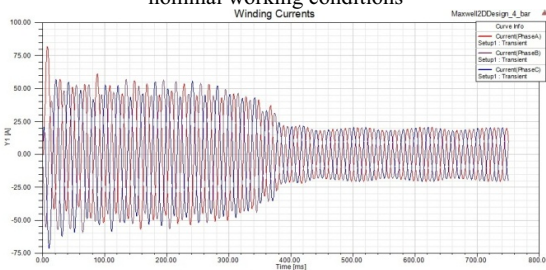**Fig. 10** Simulation results of two broken rotor bars

At this analysis, the motor has reached to nominal working conditions after 200 miliseconds. As it can be seen from the graphics, there are fluctuations on the torque and speed graphs. Also magnetic saturation areas occurs around the broken rotor bars, which can be seen at Fig. 10(a).

### 3.2.2 The effects of four broken rotor bars to the motor performance

The faulty motor with four broken rotor bar is analyzed with Maxwell-2D. As a result of analysis, the magnetic flux density during the maximum current, the current vs time, torque vs time and speed vs time graphics for the defined motor are obtained and presented at Fig. 11 (a), (b), (c) and (d) respectively.
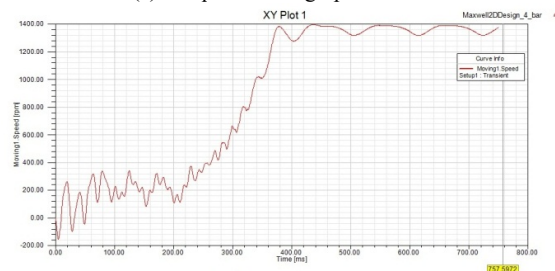

(a) The magnetic flux density during maximum current at nominal working conditions

(b) Phase current vs time
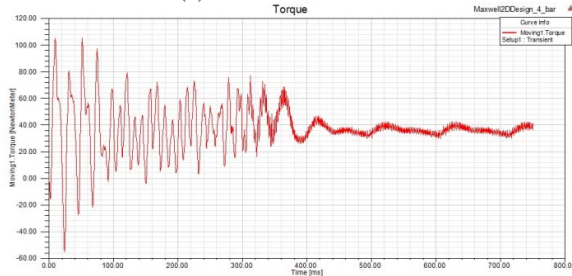
(c) Torque vs time graphic

(d) Speed vs time graphic

Fig. 11 Simulation results of four broken rotor bars

As can be seen from the graphics, the motor has reached to nominal working conditions after 400 miliseconds The start up time is almost twice of the healty motor, so motor is exposed to start up currents for longer times. The motors which starts and stops often, this situation may cause heating and overcurrent fault problems. There are fluctuations on the torque and speed as expected.

4. Conclusions

In this paper, ANSYS Maxwell 2D and RMxprt software tools are used to create a squirrel cage motor design and to analyze the effects of static eccentricity, two broken rotor bar situation and four broken rotor bar situations are simulated and the results are presented. The motor parameters and characteristics can be accurately calculated and predicted in terms of field computation and analysis results. Also it is seen that by developing the computer technology and increasing computing times, the FEM tools are becoming more useful to analyse the fault conditions which occurs in both production prossesings and the field operations, concurrently they are being used in design phases of production.

5. References

[1] Zhou Rui; Wang Qunjing; Li Guoli; Pang Cong; Fang Guanghui, "Optimal design of single-phase induction motor based on MAXWELL 2D Rmxprt," Electrical Machines and Systems (ICEMS), 2010 International Conference on , vol., no., pp.1367,1370, 10-13 Oct. 2010

[2] Qiu Changli; Cheng Jihang; Li Jingquan, "Simulation analysis of the performance of linear introduction motor in Maxwell 2D," Electrical & Electronics Engineering (EEESYM), 2012 IEEE Symposium on , vol., no., pp.360,363, 24-27 June 2012

[3] Mei-shan Jin; A-lin Hou; Chang-li Qiu; Da-chuan Chen, "A Maxwell 2D emulated analysis in the performance of linear introduction motor," Computer, Mechatronics, Control and Electronic Engineering (CMCE), 2010 International Conference on , vol.4, no., pp.348,351, 24-26 Aug. 2010

[4] Swedrowski, L.; Rusek, J., "Model and simulation tests of a squirrel - cage induction motor with oscillation of the air gap," Diagnostics for Electric Machines, Power Electronics and Drives, 2005. SDEMPED 2005. 5th IEEE International Symposium on , vol., no., pp.1,6, 7-9 Sept. 2005

[5] http://www.maintenanceworld.com